JAST, Vol. 11, No. 1, pp. 61- 75

JAST
Journal of Aerospace Science and Technology

Robust Fixed-order Gain-scheduling Autopilot Design using State-space Stability-Preserving Interpolation

H. Dehghani Firouzabadi[1] and I. Mohammadzaman[2*]

1, 2. Department of Electrical and Electronic, University of Technology Malek Ashtar

*Postal Code: 15875-1774, Tehran, Iran

Mohammadzaman@mut.ac.ir

In this paper, a robust autopilot is proposed using stable interpolation based on Youla parameterization. The most important condition of stable interpolation between local controllers is the preservation of stability so that each local controller can ensure stability for an open neighborhood around a nominal point. The proposed design used fixed-order robust controller with parameter-dependent central polynomial for each vertex of the polytope to decrease the conservation of each local controller. A stability-preserving gain-scheduled controller was designed using a newly proposed algorithm in the flight envelop for a parameter varying model. The results of simulation confirm the efficiency of the proposed method.

Keywords: Robust autopilot, stability preserving interpolation, fixed-order controller, parameter-dependent central polynomial

List of symbols

Q: Dynamic pressure
S: pursuit's reference surface
D: pursuit's diameter
X: Force applied on pursuit along body x
Y: Force applied on pursuit along body y
Z: Force applied on pursuit along body z
L: Momentum around roll axis
M: Momentum around pitch axis
N: Momentum around Yaw axis
p: Angular speed around body x axis
q: Angular speed around body y axis
r: Angular speed around body z axis
m: Mass of pursuit
Ix: Moment Inertia around x axis
Iy: Moment Inertia around y axis
Iz: Moment Inertia around z axis
δ: Angle of operator winglet
$C_{z\alpha}$: Variations of force coefficient along z due to changes of attack angle
$C_{z\delta e}$: Variations of force coefficient along z due to changes of winglet angle
C_{zq} : Variations of force coefficient along z due to changes of angular speed, q
$C_{m\alpha}$: Variations of M due to changes of attack angle
$C_{z\delta e}$: Variations of M due to changes of winglet angle
C_{zq}: Variations of M due to changes of angular speed
U: Component of speed on pursuit along x in body system
V: Component of speed on pursuit along y in body system
W: Component of speed on pursuit along z in body system
α: Attack angle
β: Lateral sleep angle
e: Elevator winglet angle
a: Eileron winglet angle
r: Rudder winglet angle

1. M.Sc.
2. Assistant Professor (Corresponding Author)

δ: Differential variable
c: Command signal

Introduction

Autopilot design is a subject in control engineering and aerospace systems which is open to research. Nonlinear dynamics, time varying parameters, uncertainty in the model, variation of flight conditions and aerodynamic coefficients can cause complicated and challenging problems in autopilot design [1-6]. In many methods developed for designing the autopilot, a certain number of nominal points on the linear model of the system are considered and a linear time invariant autopilot is designed which provides the stability and performance in local areas around the nominal point of the nonlinear system. In this condition, by moving from this nominal point, changes in the system dynamics start to grow in ways that decrease the performance and stability of the system.

Now adays, pursuits must not only have high manoeuvrability and allow the fast execution of input commands whilst preserving the stability, but also they must have a good robustness against the system parameters. Due to the simplicity and constancy of the controller, robust control methods have an advantage which results in situations where control is made possible by using these techniques, this method is preferred over the other methods of controller design. Different methods have been proposed in the design of robust controllers such as H_∞ and μ synthesis. These methods are designed in a systematic way; moreover, they involve considerations of efficiency and robustness against uncertainties and have been used in autopilot design [6-9].

These methods also have disadvantages which make them difficult to work with. First, the choice of weights has a special complexity and the process of selecting weights must be repeated several times to achieve the desired stability margin. This is a time consuming procedure and it is also uncertain whether the achieved robust stability margin is the best stability margin. Moreover, in most robust design techniques, the designed controller has a full order, so that it is equivalent to the order of the weight function plus the order of the system [10].Therefore, its use leads to challenges in practical applications such as aerospace systems. Although, there are some methods for reducing the controller order, by approximating system models or approximating the high-order controller, these methods do not guarantee the fulfilment of the desired efficiencies [11]. For this purpose, fixed order controller has been a problem on which control designer shave recently focused [12-16].In this way the order of the controller is up to the designer and the performance can be achieved with a desired stability margin. For the controller design, uncertainties of physical parameters are modelled in a polytopand the design problem is converted into a convex problem by a central polynomial and then solved withan appropriate software.

Gain-scheduling is one common method of controller design for parameter-dependent nonlinear systems, especially space systems [17-18]. A lot of research has focused on autopilot design for these systems because of the complexity of the dynamic modelling of a pursuit, such as the system uncertainty, parameter-based dynamics and nonlinear aerodynamic behaviour [19-20].

In the traditional design method for gain-scheduling, a nonlinear system becomes linear and employs local controllers at specified nominal points. Then, the linear controller is interpolated according to the existing methods in real time and concurrent with the system movement between the nominal points. There are different methods for conducting this interpolation. The advantage of these methods is that they are not conservative and an interpolated controller always exists [21-24]. The biggest disadvantage is that the stability of the final controller may not ensure a linear-based model interpolation invariant with time.

Recently, several methods have been presented for designing gain-scheduled controllers for a parameter-variant closed-loop system by preserving the stability [18,25]. Among these methods based on parameter-variant systems and guarantees for the stability of the final gain-scheduling system, there is a method of interpolation involving observers and state feedback [25]. This method is complicated because of the interpolation of the state-space matrices. Another method, in which the stability of the final gain-scheduling system is insured, is the Yula-based parameter interpolation [18]. In this method, the most important condition for interpolation is stability preservation. It means

that locally designed controllers must ensure the stability of an open neighbourhood around a nominal point and an area of common stability must exist between the two adjacent local controllers so that the interpolation is possible.

In this paper, a fixed-order robust autopilot is designed to ensure the stability and performance of the pursuit in any nominal point of the flight envelope. In the fixed order controller, a transfer function is proposed considering H_∞ norm constraints and using real positive and real bounded lemmas or small-gain theorem. Then, the numerator and denominator polynomials of this transfer function are divided by a central fixed-stable polynomial and the controllable canonical form of both transfer functions is obtained. The matrix inequality is solved using the Kalman-Yakubovich-Popov lemma assuming a common symmetrical positive matrix for its implementation. By solving this inequality, a low degree fixed-order controller is obtained. The designed controller has a high conservation caused by constant central polynomials for the vertexes of the polytopic system, which preclude linear matrix inequalities. To reduce the conservation, a variable central polynomial, called parameter-dependent central polynomial, is used. It means that a unique central polynomial is defined for each vertex of the polytopic system so that the conservation is strongly reduced and the autopilot is easier to design. In this way, the number of nominal points for the whole flight interval of the pursuit is reduced. Furthermore, the interpolation of Yula parameters has been applied for the stable interpolation between controllers which ensure stability in interpolated regions. Finally, a new systematic algorithm is proposed to design the robust autopilot while preserving the stability of a closed-loop system in the whole flight interval. The simulation results of the nonlinear system confirm the suitable performance of this autopilot.

H_∞ Fixed-Order Controller

The frequency response of the system and minimization of the H_∞ norm and robust stability margin can be written as:

$$\left\|W(s)H(s)\right\|_\infty = \left\|\frac{S(s)}{L(s)}\right\|_\infty < \gamma \qquad (1)$$

in which, *H(s)* is the output sensitivity function or sensitivity complementary function, γ is the robust stability margin, and *S(s)* and *L(s)* are two polynomials. In the small-gain theorem [10], the H_∞norm constraint in Eq.(1) is equal to the robust stability of the uncertain polynomial:

$$L(s)+\delta S(s), \quad \left\|\delta\right\|_\infty < \gamma^{-1} \qquad (2)$$

To design the fixed-order controller using a parameter-dependent central polynomial, a primary fixed-order stabilizer controller, K_0, is assumed to stabilize the polytopic system without efficiency constraints. For each vertex of this polytope, the controller concludes a closed-loop specification polynomial as the desired central polynomial [14]:

$$E_i(s) = L_i(s)\big|_{K=K_0} \qquad (3)$$

Theorem 1[14]: Consider K_0 for a given polytopic system (without an efficiency constraint). Fixed-order controller $K(s)$ becomes:

$$K(s) = \frac{y(s)}{x(s)} = \frac{y_0 s^m + y_1 s^{m-1} + ... + y_m}{s^m + x_1 s^{m-1} + ... + x_m} \qquad (4)$$

The controller stabilizes the closed-loop system containing uncertainties and satisfies the H_∞ efficiency condition in Eq. (1) for the polytopic system if the symmetrical matrix $P_i = P_i^T$ and scalar τ_i and matrix Q exist, so that $i = 1,...,q$ produces:

$$\begin{bmatrix} \begin{bmatrix} 0 & C_{li}^T & -C_{si}^T \\ C_{li} & D_{li}+D_{li}^T-\tau_i & -D_{si}^T \\ -C_{si} & -D_{si} & \tau_i\gamma^2 \end{bmatrix} & \begin{bmatrix} -P_i \\ 0 \\ 0 \end{bmatrix} \\ \begin{bmatrix} -P & 0 & 0 \end{bmatrix} & 0 \end{bmatrix} + \begin{bmatrix} \begin{bmatrix} A_i^T \\ B^T \\ 0 \end{bmatrix} \\ -I \end{bmatrix} Q^T + Q\begin{bmatrix} \begin{bmatrix} A_i & B & 0 \end{bmatrix} & -I \end{bmatrix} > 0 \qquad (5)$$

in which (A_i, B, C_{li}, D_{li}) and (A_i, B, C_{si}, D_{si}) are controllable canonical realizations of the transfer functions $\frac{L_i(s)}{E_i(s)}$ and $\frac{S_i(s)}{E_i(s)}$, respectively.

Gain-Scheduled Controller Using Stability-Preserving Interpolation

Definition 1 [18]: A parameter-variant linear system $\Sigma(\rho)$ is assumed in which $x(t)\in R^n$ is the state matrix, $u(t)\in R^m$ is the control signal, $e(t)\in R^{p_e}$ is the output, $w(t)\in R^{m_w}$ is the external signal, and $y(t)\in R^p$ is the measured signal:

$$\begin{cases}\dot{x}(t)=F(\rho)x(t)+G_1(\rho)w(t)+G_2(\rho)u(t)\\ e(t)=H_1(\rho)x(t)+J_{11}(\rho)w(t)+J_{12}(\rho)u(t)\\ y(t)=H_2(\rho)x(t)+J_{21}(\rho)w(t)\end{cases} \quad (6)$$

in which $\rho\in\Gamma\subset R^l$ and Γ is a closed set of the domain of gain-scheduled variables.
Assume $\Lambda_1,...,\Lambda_\rho$ as time-invariant linear controllers for constant values $\rho_1,...,\rho_q\in\Gamma$, so that each controller can preserve the stability of its corresponding time-invariant linear system $\Sigma(\rho_i)$.

Preserving stability is the most important condition in a stability-preserving interpolation for time-invariant linear controllers. It must exist in open neighborhood U_i that includes ρ_i to stabilize the local controller Λ_i, so that Λ_i stabilizes the system $\Sigma(\rho)$ for all $\rho\in U_i$, i = 1,...,q. Assuming satisfaction of condition $\Gamma\subset\bigcup_{i=1}^{q}U_i$, the local controller covers all scheduling space. Hypothesis 1 achieves the stability-preserving conditions.

Hypothesis 1[26]: Assume the local controllers $\Lambda_1,...,\Lambda_q$ as designed at points $\rho_1,...,\rho_q\in[\rho_1,\rho_q]\subset R$ and that their existing open intervals $U_1,...,U_q$, so that each U_i includes ρ_i and Λ_i for each $\rho\in U_i$, and $\Gamma\subset\bigcup_{i=1}^{q}U_i$ stabilizes system $\Sigma(\rho)$. Since stability-preserving interval U_i is open, there are intervals $[a_i,b_i]\subset U_i\cup U_{i+1}$, $i=1,...,q-1$ so that controllers Λ_i and Λ_{i+1} stabilize system $\Sigma(\rho)$ for all $\rho\in[a_i,b_i]$.
Theorem 2 offers a local controller interpolation and shows that the interpolated controller can stabilize the given system.

Theorem 2[18]: Assume a parameter-variant linear system $\Sigma(\rho)$ with dimension *n* in Eq. (6) and parameter $\rho\in[a,b]$.Assume time-invariant linear controllers Λ_1 and Λ_2 with dimensions n_k so that Λ_1 preserves the stability of system $\Sigma(\rho)$ in $\rho\in[a,d)$ and Λ_2 preserves the stability of system $\Sigma(\rho)$ in $\rho\in(c,b]$ while stability-preserving is satisfied. Parameter-variant $\Lambda(\rho)$ with dimension $2n+n_k$ exists where $\Sigma(\rho)$ is stable for all $\rho\in[a,b]$ and $\Lambda(a)$ and $\Lambda(b)$ have equal transfer functions, Λ_1 and Λ_2, respectively. The coefficients of matrix $\Lambda(\rho)$ are continuous functions of variable ρ.

In the stable interpolation of the state-space matrix of the parameter-variant linear system and time-invariant linear controller, linear fractional transformations used to design the interpolated controller. Local controllers can have any degrees or dimensions, but the degrees and dimensions of two adjacent controllers with a common area must be equal. The process of finding the interpolated controller between two adjacent controllers with a common area [14] is:

1. Consider a parameter-variant linear system for Eq. (6). Local time-invariant autopilot state-space realizations (A_i, B_i, C_i, D_i) have order n_k so that autopilot Λ_1 can preserve the stability of $\Sigma(\rho)$ in interval $\rho\in[a,d)$ and autopilot Λ_2 can preserve the stability of $\Sigma(\rho)$ in interval $\rho\in(c,b]$ (c<d) and stability-preserving is satisfied. In interval [c,d], $0<\rho<1$ ($c=0, d=1$).
2. The closed-loop stable matrix $\tilde{A}_i(\rho)$ is:
$$\tilde{A}_i(\rho)=\begin{bmatrix}F(\rho)-G_2(\rho)D_iH_2(\rho) & G_2(\rho)C_i\\ -B_iH_2(\rho) & A_i\end{bmatrix} \quad (7)$$
3. Using $W_1(\rho)$ and $W_2(\rho)$ as positive symmetrical matrices, the following linear

matrix inequality is solved and matrices $W_1(\rho)$ and $W_2(\rho)$ will be obtained for all ρ.

$$\begin{aligned}&\tilde{A}_1^T(\rho)W_1(\rho)+\\&W_1(\rho)\tilde{A}_1(\rho)<-I,\qquad \rho\in[a,d)\end{aligned}\tag{8}$$

$$\begin{aligned}&\tilde{A}_2^T(\rho)W_2(\rho)+\\&W_2(\rho)\tilde{A}_2(\rho)<-I,\qquad \rho\in(c,b]\end{aligned}\tag{9}$$

4. Matrices L_i and K_i are obtained using the following linear matrix inequalities:

$$\begin{aligned}&(F_i(\rho)+G_{2i}(\rho)K_i(\rho))^T R_i^{-1}(\rho)+\\&R_i^{-1}(\rho)(F_i(\rho)+G_{2i}(\rho)K_i(\rho))<-I\end{aligned}\tag{10}$$

$$\begin{aligned}&(F_i(\rho)+L_i(\rho)H_{2i}(\rho))^T S_i(\rho)+\\&S_i(\rho)(F_i(\rho)+L_i(\rho)H_{2i}(\rho))<-I\end{aligned}\tag{11}$$

where $R_i(\rho), S_i(\rho)\in R^{n\times n}$, $i=1,2$ is:

$$\begin{aligned}&W_i(\rho)=\begin{bmatrix}S_i(\rho) & N_i(\rho)\\ N_i^T(\rho) & P_i(\rho)\end{bmatrix},\\&W_i^{-1}(\rho)=\begin{bmatrix}R_i(\rho) & M_i(\rho)\\ M_i^T(\rho) & Q_i(\rho)\end{bmatrix}\end{aligned}\tag{12}$$

where $P_i(\rho), Q_i(\rho)\in R^{n_k}$, $i=1,2$.

Matrices L and K are defined as:

$$\begin{aligned}&L(\rho)=\begin{cases}L_1(\rho) & \rho\in[a,c)\\ S^{-1}(\rho)((1-\rho)S_1(\rho)L_1(\rho)+\rho S_2(\rho)L_2(\rho)) & \rho\in[c,d]\\ L_2(\rho) & \rho\in(d,b]\end{cases}\\&K(\rho)=\begin{cases}K_1(\rho) & \rho\in[a,c)\\ ((1-\rho)K_1(\rho)R_1(\rho)+\rho K_2(\rho)R_2(\rho))R^{-1}(\rho) & \rho\in[c,d]\\ K_2(\rho) & \rho\in(d,b]\end{cases}\end{aligned}\tag{13}$$

Where:

$$\begin{cases}S(\rho)=(1-\rho)S_1(\rho)+\rho S_2(\rho)\\ R(\rho)=(1-\rho)R_1(\rho)+\rho R_2(\rho)\end{cases}\tag{14}$$

5. Define the following matrices as:

$$\begin{aligned}&\tilde{B}_i(\rho)=\begin{bmatrix}-L(\rho)+G_2(\rho)D_i\\ -B_i\end{bmatrix}\\&\tilde{C}_i(\rho)=\begin{bmatrix}-K(\rho)-D_iH_2(\rho) & C_i\end{bmatrix},\\&\tilde{D}_i(\rho)=D_i\end{aligned}\tag{15}$$

6. $\tilde{A}_w(\rho)$ is:

$$\begin{aligned}&\tilde{A}_w(\rho)=\tilde{W}^{-1}(\rho)\\&\left((1-\rho)W_1(c)\tilde{A}_1(c)+\rho W_2(d)\tilde{A}_2(d)\right)\end{aligned}\tag{16}$$

Where:

$$\tilde{W}(\rho)=(1-\rho)W_1(c)+\rho W_2(d)\tag{17}$$

Eq. (16) is stable for all $\rho\in[a,b]$. In practice, matrices $W_1(\rho)$ and $W_2(\rho)$ are considered constant to simplify the solution to the equations. In this case, the interpolation is converted to a stable linear interpolation and Eq. (16) is written as:

$$\tilde{A}_w(\rho)=(1-\rho)\tilde{A}_1(c)+\rho\tilde{A}_2(d)$$

Obtain matrices $\tilde{A}(\rho)$ ، $\tilde{B}(\rho)$ ، $\tilde{C}(\rho)$ and $\tilde{D}(\rho)$ as:

$$\tilde{A}(\rho)=\begin{cases}\tilde{A}_1(\rho) & \rho\in[a,c)\\ \tilde{A}_w(\rho) & \rho\in[c,d]\\ \tilde{A}_2(\rho) & \rho\in(d,b]\end{cases}\tag{18}$$

$$\tilde{X}(\rho)=\begin{cases}\tilde{X}_1(\rho) & \rho\in[a,c)\\ \tilde{X}_w(\rho)=(1-\rho)\tilde{X}_1(c)+\rho\tilde{X}_2(d) & \rho\in[c,d]\\ \tilde{X}_2(\rho) & \rho\in(d,b]\end{cases}\tag{19}$$

where matrices $\tilde{B}(\rho)$ ، $\tilde{C}(\rho)$ and $\tilde{D}(\rho)$ are obtained by replacing X.

7. Defining systems $J(\rho)$ and $Q(\rho)$ as:

$$\begin{aligned}J(\rho)&\overset{\Delta}{=}\begin{cases}\dot{x}(t)=(F(\rho)+G_2(\rho)K(\rho)+L(\rho)H_2(\rho))x(t)\\ -L(\rho)w(t)+G_2(\rho)u(t)\\ e(t)=K(\rho)x(t)+u(t)\\ y(t)=-H_2(\rho)x(t)+w(t)\end{cases}\\&=\begin{cases}\dot{x}(t)=A_J(\rho)x(t)+B_{1J}(\rho)w(t)+B_{2J}(\rho)u(t)\\ e(t)=C_{1J}(\rho)x(t)+D_{11J}(\rho)w(t)+D_{12J}(\rho)u(t)\\ y(t)=C_{2J}(\rho)x(t)+D_{21J}(\rho)w(t)+D_{22J}(\rho)u(t)\end{cases}\end{aligned}\tag{20}$$

$$Q(\rho)\overset{\Delta}{=}\begin{cases}\dot{z}(t)=\tilde{A}(\rho)z(t)+\tilde{B}(\rho)y(t)\\ u(t)=\tilde{C}(\rho)z(t)+\tilde{D}(\rho)y(t)\end{cases}\tag{21}$$

Obtains an interpolated controller using linear fractional transformational:

$$F_l(J(\rho),Q(\rho))\overset{\Delta}{=}\begin{cases}\dot{x}(t)=\hat{A}(\rho)x(t)+\hat{B}(\rho)u(t)\\ y(t)=\hat{C}(\rho)x(t)+\hat{D}(\rho)u(t)\end{cases}\tag{22}$$

where [27]:

$$\hat{A}(\rho)=\begin{bmatrix} A_J(\rho)+B_{2J}(\rho)\tilde{D}(\rho)C_{2J}(\rho) & B_{2J}(\rho)\tilde{C}(\rho) \\ \tilde{B}(\rho)C_{2J}(\rho) & \tilde{A}(\rho) \end{bmatrix}$$
$$\hat{B}(\rho)=\begin{bmatrix} B_{1J}(\rho)+B_{2J}(\rho)\tilde{D}(\rho)D_{12J}(\rho) \\ \tilde{B}(\rho)D_{21J}(\rho) \end{bmatrix}$$
$$\hat{C}(\rho)=\begin{bmatrix} C_{1J}(\rho)+D_{12J}(\rho)\tilde{D}(\rho)C_{2J}(\rho) & D_{12J}(\rho)\tilde{C}(\rho) \end{bmatrix}$$
$$\hat{D}(\rho)=\begin{bmatrix} D_{11J}(\rho)+D_{12J}(\rho)\tilde{D}(\rho)D_{21J}(\rho) \end{bmatrix} \quad (23)$$

To preserve the stability of the parameter-variant nonlinear system, ρ must be constrained as a bound on the variation rate of the gain-scheduling variable. $\rho(t)$ is considered to be an external continuous signal with a value from set Γ.

Theorem 3[26]: Consider interpolated controller $\Lambda(\rho)$ in the state-space from Hypothesis (1). If $W(\rho)$ is a symmetrical and piece-wise smooth positive definite matrix function:

$$\hat{A}^T(\rho)W(\rho)+W(\rho)\hat{A}(\rho)<-I,\ \rho\in[\rho_1,\rho_2] \quad (24)$$

Closed-loop matrix $\tilde{A}(\rho)=\begin{bmatrix} F(\rho) & G_2(\rho)C(\rho) \\ B(\rho)H_2(\rho) & A(\rho) \end{bmatrix}$ is stable (without considering input) for $\rho(t)\in[\rho_1,\rho_2]$, if:

$$|\dot{\rho}(t)|<\left\|\frac{\partial}{\partial\rho}W(\rho(t))\right\|^{-1},\ t\geq 0 \quad (25)$$

The above theorem states that, if condition (25) is satisfied for the rate of gain-scheduling, the time-variant nonlinear system will be stabilized by the interpolated controller from linear fractional transformation (20) and (21).

DOF Pursuit Equations

Assuming aerodynamic symmetry of a rolling channel and a low rate of variation for rolling angle (ρ), the equations for apursuit with 6 DOF are [28]:

$$\begin{bmatrix} X \\ Y \\ Z \end{bmatrix}=m\begin{bmatrix} (\dot{U}+qW-rV) \\ (\dot{V}+rU) \\ (\dot{W}-qU) \end{bmatrix},\qquad \begin{bmatrix} L \\ M \\ N \end{bmatrix}=\begin{bmatrix} I_x\dot{p} \\ I_y\dot{q} \\ I_z\dot{r} \end{bmatrix} \quad (26)$$

The aerodynamic forces and momentums of the above equations are [24]:

$$\begin{aligned} Y&=QS\left(C_{y_\beta}\beta+C_{y_{\delta r}}\delta_r+C_{y_r}\cdot\frac{D}{2U}r\right)\\ Z&=QS\left(C_{z_\alpha}\alpha+C_{z_{\delta e}}\delta_e+C_{z_q}\cdot\frac{D}{2U}q\right)\end{aligned} \quad (27)$$

$$\begin{aligned} L&=QSD\left(C_{l_{\delta a}}\delta a+C_{l_p}\cdot\frac{D}{2V}p\right)\\ M&=QSD\left(C_{m_\alpha}\alpha+C_{m_{\delta e}}\delta_e+C_{m_q}\cdot\frac{D}{2U}q\right)\\ N&=QSD\left(C_{n_\beta}\alpha+C_{n_{\delta r}}\delta_e+C_{n_r}\cdot\frac{D}{2U}r\right)\end{aligned} \quad (28)$$

Since there is no control on acceleration along the *x* axis the *n* body coordinate, the force applied along the*x* axis in Eq. (27) is not analyzed.

Usually, two loops are used to design an autopilot for a pursuit. The first loop is for angular speed and the second is for linear acceleration. The transfer function of angular speed of pitch by displacement of the vertical rudder $(\frac{q(s)}{\delta_e(s)})$ and the transfer function of acceleration along the *z* axis by angular speed $(\frac{a_z(s)}{q(s)})$ is written as follows after linearization and simplification with 6 DOF [24]:

$$\frac{q(s)}{\delta e(s)}=\frac{M_{\delta e}s+(Z_{\delta e}M_\alpha-Z_\alpha M_{\delta e})}{s^2-(M_q+Z_\alpha/V)s+((Z_\alpha M_q-M_\alpha Z_q)/V-M_\alpha)} \quad (29)$$

$$\frac{a_z(s)}{q(s)}=\frac{Z_{\delta e}s^2+(M_{\delta e}Z_q-Z_{\delta e}M_q)s+(Z_\alpha M_{\delta e}-Z_{\delta e}M_\alpha)}{s^2-(M_q+Z_\alpha/V)s+((Z_\alpha M_q-M_\alpha Z_q)/V-M_\alpha)} \quad (30)$$

The coefficients of the above equations are:

$$Z_q=\frac{SQDC_{z_q}}{m},\ M_{\delta_e}=\frac{SQDC_{m_{\delta e}}}{I_y},\ M_\alpha=\frac{SQDC_{m_\alpha}}{I_y}$$
$$Z_{\delta_e}=\frac{SQC_{z_{\delta e}}}{m},\ Z_\alpha=\frac{SQC_{z_\alpha}}{m},\ M_q=\frac{SQD^2C_{m_q}}{I_yV} \quad (31)$$

Fig. 1 shows changes in the aerodynamic coefficients for attack angle and mach in the proposed non-linear pursuit model. Fig. 2 shows the proposed linear model for design of the controller. The internal loop is stabilized by the selection of a suitable value for K_q as a negative

number between 0 and –1. The transfer function of the actuator is:

$$G_{act} = \frac{\delta_e(s)}{\delta_c(s)} = \frac{100^2}{s^2 + 160s + 100^2} \qquad (32)$$

The external loop is for control of the linear acceleration. The design of the autopilot is to have controller *K*in order to ensure the stability and efficiency of the closed-loop system for all flight intervals.

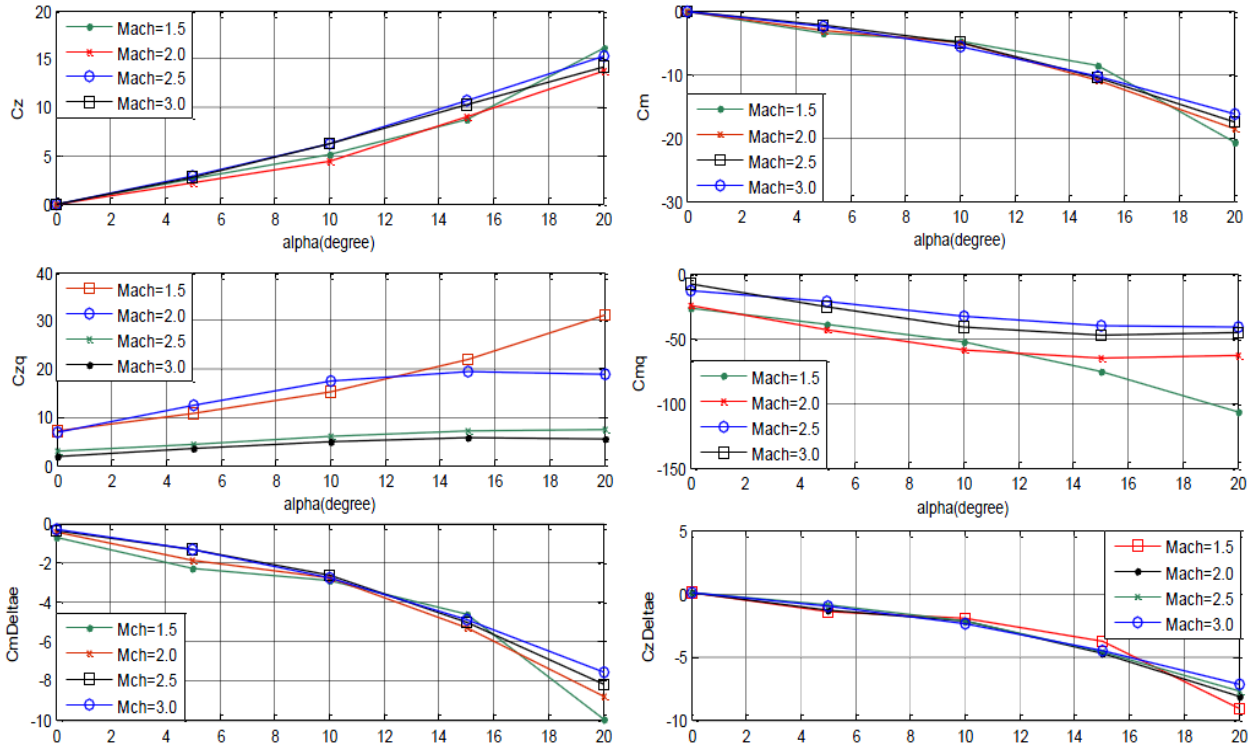

Figure 1. Changes of aerodynamic coefficients by mach and attack angle

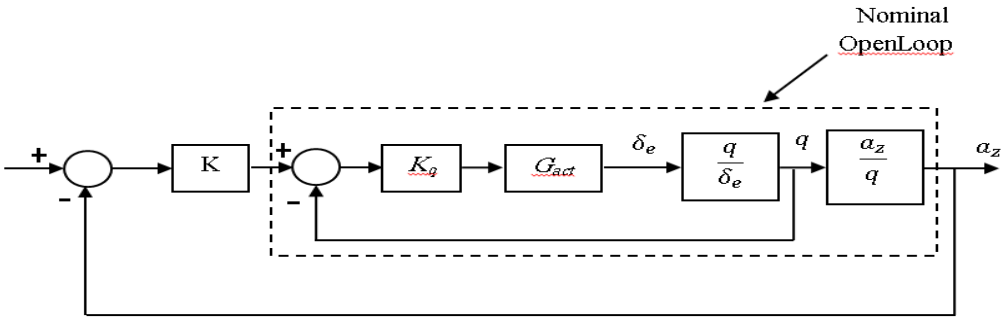

Figure 2. The linear model of system in pitch channel and its autopilot

Autopilot Design and Results of Simulation

A fixed-order robust autopilot was designed assuming the parameter-dependent central polynomial using the transfer functions from Section 4. The gain-scheduled autopilot variables were based on the measurable pursuit variables of acceleration, dynamic pressure, and mach. Selection of these variables as gain-scheduling variables created a 3×3 sophisticated table. To remove this sophistication, variables with the most effect on the system were selected. Dynamic pressure, *Q*, which has the most effect on the system, was selected to obtain the coefficients of the transfer functions.

Aerodynamic transfer functions depended on Q and the gain-scheduling variable was also Q ($\rho = Q$).The attack angle and mach were averaged for the total flight interval to obtain the transfer functions. The dynamic pressure variable was used as the gain-scheduling variable. The dynamic pressures interval on the pursuit was 30000<Q<250000, which is equal to 0<h<14 km in height. The algorithm to systematically select the dynamic pressure interval and design the controller for that interval as:

1. Assume minimum and maximum dynamic pressure in the flight interval and divide the dynamic pressure equally (e.g., by 1000).
2. Begin movement at maximum dynamic pressure. Calculate the aerodynamic coefficients in Eq. (31) for each segment to obtain transfer functions $\frac{q(s)}{\delta_e(s)}$ and $\frac{a_z(s)}{q(s)}$ .First stabilize the internal loop (angular speed loop) using a suitable gain $K_q$as a negative number between 0 and –1 (Fig. 2). Then calculate open-loop transfer function $\frac{a_z(s)}{\delta_e(s)}$.
3. The maximum and minimum of each s coefficient in the transfer function is assumed to obtain the transfer function coefficients for the dynamic pressure from Section 2. The n coefficients are used to obtain 2^n new transfer functions, each forming one vertex of the polytopic system. For example, the transfer function of the pitchchannel has 3 coefficients in its numerator and 5 coefficients in its denominator, which results in 128 systems from the minimum and maximum number of coefficients (no zero coefficient).
4. Assume a fixed-order stabilizing controller, K_0, to stabilize the polytopic system without efficiency constraints. This controller can be fixed-order using the constant central polynomial method without the efficiency constraints described by Khatibi et al.(2010) [11]. This controller produces a closed-loop specification polynomial similar to Eq. (3) for each vertex of the polytope.
5. The sensitivity weight function is formed and the central polynomial for each vertex is calculated using Eq. (3). The central polynomial must be unique.
6. Form polynomials $S(s)$ and $L(s)$ using Eq. (1) in the polytopic state and divide them by the central polynomials from Step 4 to obtain their controllable canonical realizations. The linear matrix inequalities from Theorem 1 are solved in the polytopic state and the controller is obtained.
7. Return to Step 1 and repeat the algorithm in increments of the dynamic pressure interval. Continue until the linear matrix inequalities are infeasible. The stability of linear system is achieved with the solution of this inequality. Fig. 3 shows the flowchart of this algorithm.
8. The efficiency criteria for high dynamic pressure (>70000) were $M_p < 10\%$, $t_s < 1\,s$, and $t_r < 0.7\,s$ .For low dynamic pressures (<70000),they were $M_p < 10\%$, $t_s < 2\,s$, and $t_r < 1.5s$. Table 1 shows the dynamic pressure intervals and fixed-order autopilot designed using this method.

Tables 1 and 2 indicate that the number of local controllers decreased for the parameter-variant central polynomial method (3) when compared to the constant central polynomial method (6). This is the result of the decrement of conservation in the parameter-dependent central polynomial method presented in Table 2.

Table 1. Dynamic pressure intervals and fixed-order robust local autopilots for each interval by parameter-dependent central polynomial

Dynamic pressure interval		**Fixed-order robust local autopilot**
First interval	115,000 - 250,000	$\frac{-0.0030946(s+16.46)(s+0.5397)}{s(s+0.5802)}$
Second interval	62,000 - 117,000	$\frac{-0.0070294(s+7.929)(s+0.4623)}{s(s+0.5693)}$
Third interval	30,000 - 64,000	$\frac{-0.0081309(s+4.849)(s+0.5034)}{s(s+0.5184)}$

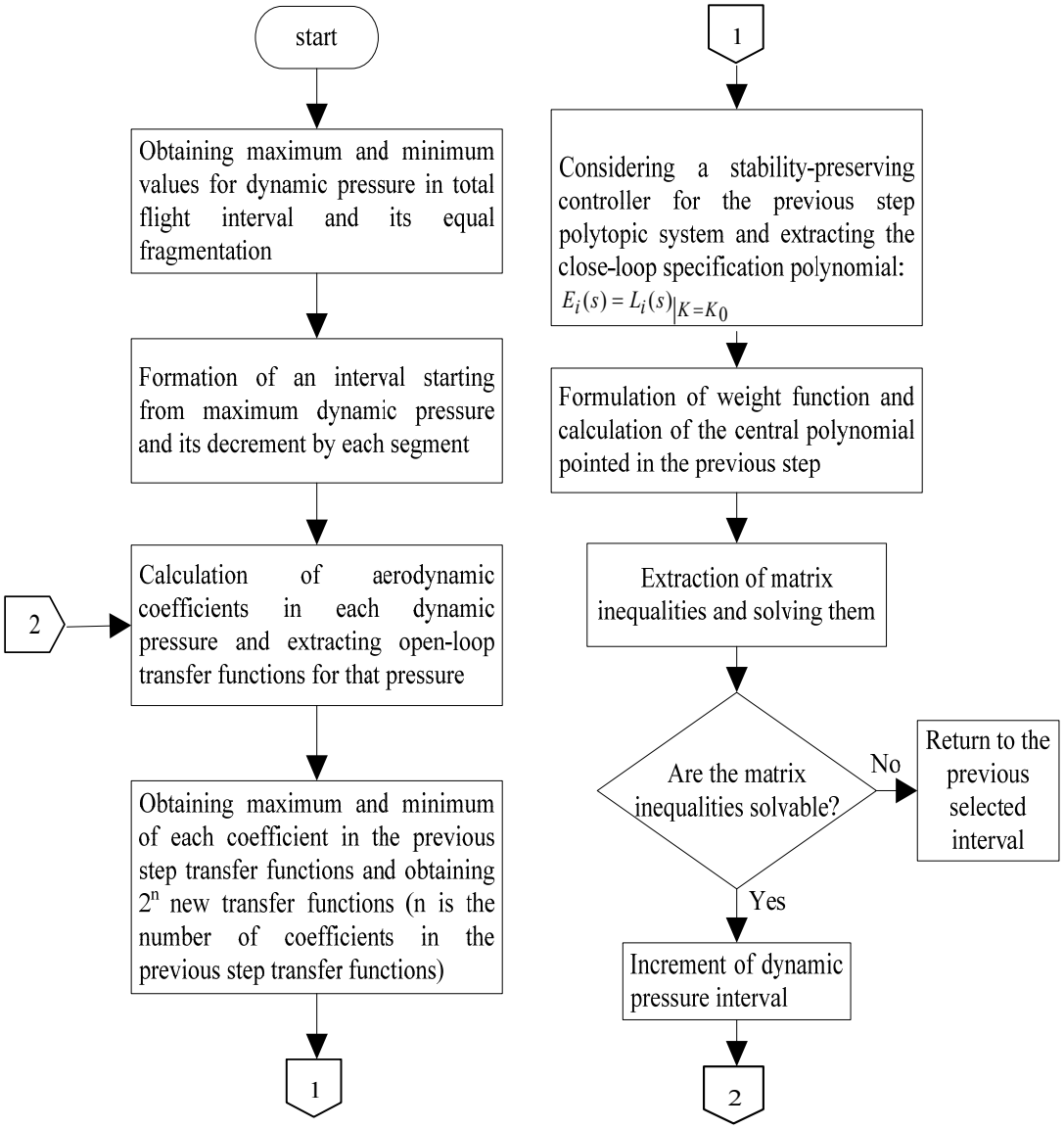

Figure 3. Flowchart of fixed-order autopilot designing process using parameter-dependent central polynomial.

Table 2. Fixed-order robust local autopilots by fixed central polynomial method

	1'st interval	2'nd interval	3'd interval	4'th interval	5'th interval	6' interval
Q	145000→250000	94000→147000	68000→96000	53000→70000	38000→55000	30000→40000
Controller	$-0.005428\frac{s+13.51}{s(s+0.9767)}\times(s+0.9273)$	$-0.0062323\frac{s+11.25}{s(s+0.9371)}\times(s+.7756)$	$-0.0074167\frac{s+8.797}{s(s+0.3474)}\times(s+.0.361)$	$-0.0095875\frac{s+6.295}{s(s+0.3861)}\times(s+0.4079)$	$-0.0096962\frac{s+6.244}{s(s+0.4978)}\times(s+0.4366)$	$-0.010029\frac{s+5.246}{s(s+0.4519)}\times(s+0.4177)$

Interpolated local autopilots were obtained using the algorithm in Section 3. The equal response of the autopilots to local autopilots (input/output response) is the key element of this system. To test this assertion, a nominal open-loop transfer function in dynamic pressure interval 1 was assumed with a common dynamic pressure between intervals 1 and 2 and satisfying

stability-preserving. The point selected for interpolation as 116000; its pitch channel is an open-loop transfer function (Fig. 2) in which the input is pitch channel angular speed and the output is acceleration along the body of the z axis:

$$G\_OpenLoop = \frac{1.2629*10^5}{(s+13.05)\,(s+9.073)} \times \frac{(s-24.12)\,(s+21.01)}{(s^2+141.2s+7364)} \quad (33)$$

Matrices $\tilde{A}_1(\rho)$ and $\tilde{A}_2(\rho)$ were obtained using local autopilots from Eq. (7). Matrices $\tilde{A}_w(\rho)$ were the n obtained using Eq. (16). $\tilde{B}_w(\rho)$, $\tilde{C}_w(\rho)$ and $\tilde{D}_w(\rho)$ were obtained using Eq. (19). For example, matrix $\tilde{A}(\rho)$ was:

$$\tilde{A}_w(\rho) = \tilde{W}^{-1}(\rho)\left(\frac{117000-116000}{117000-115000} W_1 \tilde{A}_1(115000) + \frac{116000-115000}{117000-115000} W_2 \tilde{A}_2(117000)\right) \quad (34)$$

Matrices W_1 and W_2 were constant and symmetrical in interval [115000, 117000]. The interpolated autopilot transfer function was calculated using Eqs. (20)-(23). The interpolated autopilot transfer function for dynamic pressure 116000 was (index I is the interpolated autopilot):

$$K_I = \frac{639.3\,(s+1.302*10^5)\,(s-1.972*10^4)}{(s+2.982*10^4)\,(s+1.405*10^5)\,(s+84.4)} \times \frac{(s+82.27)\,(s+61.82)\,(s+21.01)}{(s+0.5336)\,(s+13.76)(s^2+8.261s+34.5)} \times \frac{(s+15.79)(s-24.12)\,(s+0.5397)}{(s+59.48)(s^2+16.63s+201.7)} \times \frac{(s^2+16.81s+204.3)\,(s+14.99)\,(s+10.55)}{(s^2+141.3s+6965)(s+14.77)(s+10.52)} \quad (35)$$

Fig. 4 shows the results of the stepped response of the closed-loop system for the interpolated and local autopilots. As seen, the responses of the closed-loop systems in both autopilots were equivalent.

The constant matrix $W(\rho)$ for the interval between both local controllers was obtained. Variation rate $\rho(t)$ is infinite using Eq. (25) and there is no constraint on it, which is an advantage in the design of an autopilot.

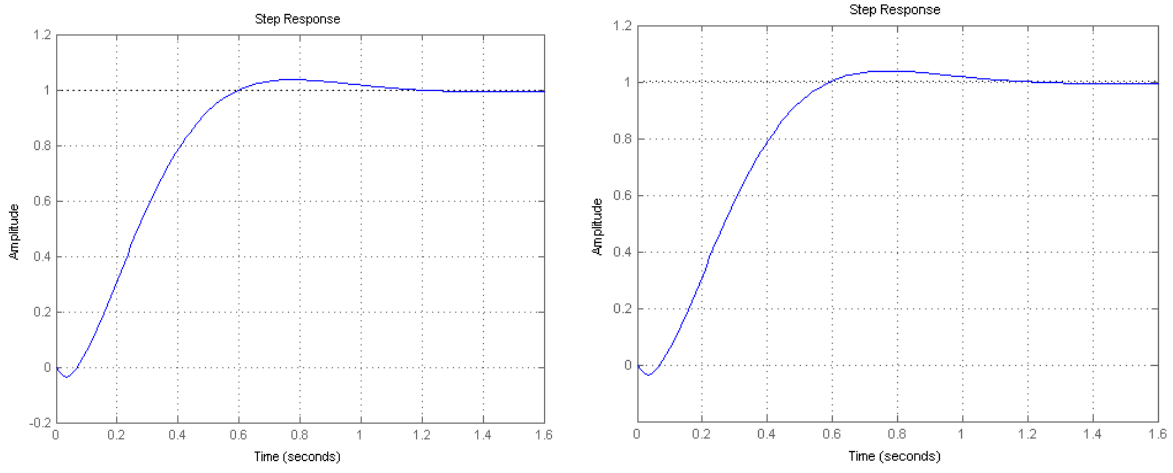

A B

Figure 4. Step response of closed-loop system by interpolated (A) and local (B) autopilots in dynamic pressure 116000.

The gain-scheduled autopilot is simulated using the non-linear model to illustrate that efficiency criteria for the flight path were satisfied. Local autopilots are designed using the parameter-variant central polynomial for interpolation of the nonlinear model. The pursuit astail-controlled structure and therefore the system is a non-minimum phase. Early in the change process in the reference acceleration, pursuit acceleration moved opposite to the direction of reference acceleration and then toward it. Fig. 5 shows the reference acceleration

order compared to the real acceleration of a pursuit. As shown, the efficiency criteria were satisfied. Fig. 6 shows the changes in input control signal by time and indicates that changes in the wing angle were desirable and acceptable.

Fig. 7 shows the dynamic pressure and height curves for different flight times. The dynamic pressure increased up to 240000 and all nominal points were stimulated according to the order of input acceleration. Switching between the local controllers was evident. Since the aerodynamic coefficients are usually extracted experimentally and numerically and may be inaccurate, the gain-scheduled autopilot for 25% tolerance for each aerodynamic coefficient was examined. Fig. 8 shows an efficiency criterionof25% tolerance and indicates that the input order was closely followed.

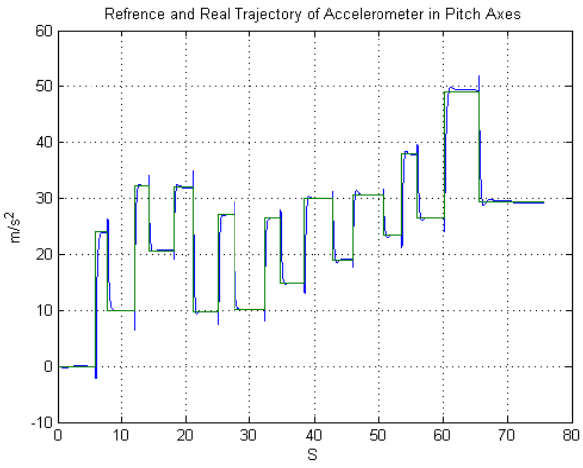

Figure 5. Pursuit acceleration in pitch axes.

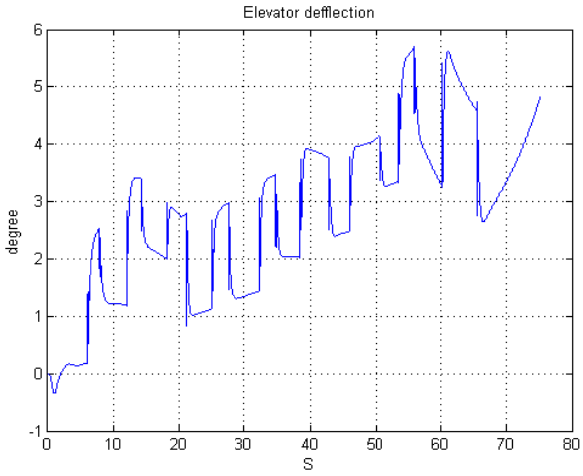

Figure 6. Input control signal.

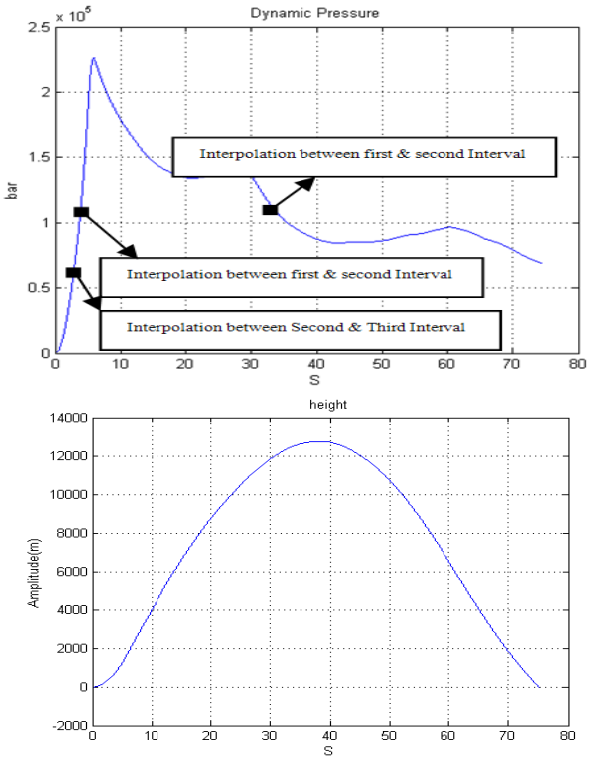

Figure 7. Changes in dynamic pressure and height by flight time.

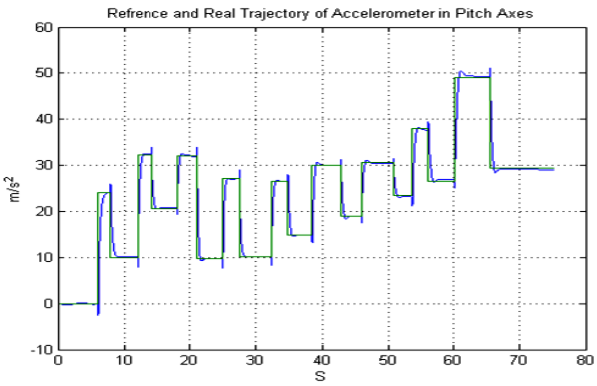

Figure 8. Pursuit acceleration with 25% tolerance of aerodynamic coefficients.

Conclusion

A stable interpolation method in state-space is proposed and used to design a pursuit autopilot. This method interpolates local autopilots and ensures stability of the parameter-variant system. A new algorithm is proposed employing the fixed-order controller design method for local autopilots at nominal points with SSP between adjacent autopilots. The fixed-order robust controller design method uses the H_∞ approach in

which a parameter-dependent central polynomial is used with lower conservation than in the constant type. The results of simulation with 6 DOF showed a desirable performance for the final gain-scheduled controller.

References

[1] Robert T. Reichert. "Dynamic Scheduling of Modern- Robust-Control Autopilot Designs for Missiles", *Conference on Decision and Control, Brighton, England*, 1991.

[2] Seong Nam, H., Hwan Kim, S., ho Song, Ch. JoonL you. "A Robust Nonlinear Control Approach to Missile Autopilot Design", *Proceedings of the 40th SICE Annual Conference*, 2001.

[3] Huang, J., Lin, C.F., Cloutier, J.R. and Evers J.H., "Robust Feedback Linearization Approach to Autopilot Design," *First IEEE Conference on Control Applications*, 1992.

[4]B. Brugarolas, P., Fromion, V., Safonov, M.G., "Robust Swithing Missile Autopilot," *Proceedings of the American Control Conference,* Philadelphia, Pennsylvania June 1998.

[5] Mattei, G. and Monaco, S., "Nonlinear Autopilot Design for an Asymmetric Missile using Robust Back Stepping Control," *Journal of Guidance, Control, and Dynamics*, Vol. 37, No. 5, 2014, pp. 1462-1476.

[6] Mahmood, A., Kim, Y. and Park, J., "Robust H∞ Autopilot Design for Agile Missile with Time-Varying Parameters," *IEEE Transactions on Aerospace and Electronic Systems*, Vol. 50, Issue 4, 2014.

[7] Yang, S.M., Mears, B.C. and Poolla, K., "Application of H∞ Control to Pitch Autopilot of Missiles," *IEEE Transactions on Aerospace and Electronic Systems*, Vol. 32, No. 1, 1996, pp. 426-433.

[8] Buschek, H., "Full Envelope Missile Autopilot Design Using Gain Scheduled Robust Control," *Journal of Guidance, Control and Dynamics*, Vol. 22, No. 1, 1999.

[9] Reichert, R.T., "Robust Autopilot Design using μ-Synthesis," *American Control Conference*, May 1990, pp. 2368 – 2373.

[10] Zhou, K. and Doyle, J. C., *Essentials of Robust Control*, Upper Saddle River, NJ: Prentice-Hall, 1998.

[11] Anderson, B.D.O. and Liu, Y., "Controller Reduction: Concepts and Approaches," *IEEE Transactions on Automatic Control*, Vol. 34, No. 8, 1989, pp. 802-812.

[12] Henrion, H., Sebek, M. and Kuˇcera, V., "Positive Polynomials and Robust Stabilization With Fixed-Order Controllers," *IEEE Transaction on Automatic Control*, Vol. 48, No. 7, 2003, pp. 1178-1185.

[13] Khatibi, H. and Karimi, A. R., "H∞ Controller Design Using an Alternative to Youla Parameterization," *IEEE Transaction on Automatic Control*, Vol. 55, No. 9, 2010, pp. 2119-2123.

[14] Sadeghzadeh, A., "Fixed- order H∞ Controller Design for Systems with Polytopic Uncertainty," *18th IFAC World Congress Milano (Italy),* August 28 - September 2, 2011.

[15] Sadeghzadeh, A. "Fixed-structure H_infinity Controller Design for Systems with Polytopic Uncertainty: An LMI Solution," *Asian Journal of Control*, Vol. 6, No. 6, 2014, pp. 1859-1868.

[16]Parastvand, H, Khosrowjerdi, M.J., "Controller Synthesis Free of Analytical Model: Fixed-order Controllers," *International Journal of Systems Science*, Vol. 46, Issue 7, 2015.

[17] Saussi´, D., Saydyand, L. and Akhrif, O., "Gain Scheduling Control Design for a Pitch-Axis Missile Autopilot," *AIAA Guidance, Navigation and Control Conference and Exhibit*, Honolulu, Hawaii, 18-21 August 2008, pp. 1-16.

[18] Stilwell, D.J., "State Space Interpolation for a Gain Scheduled Autopilot," *Journal of Guidance, Control and Dynamics*, Vol. 24, 2001, pp. 460 465.

[19] Reichert, T.R, "Dynamic Scheduling of Modern-robust-Control Autopilot Designs for Missiles," *IEEE Control Systems Magazine,* Vol. 12, No. 5, 1992, pp. 35-42.

[20] Buschek, H., "Full Envelope Missile Autopilot Design Using Gain Scheduled Robust Control", *Journal of Guidance, Control and Dynamics*, Vol. 22, No. 1, 1999, pp.115 122.

[21] Kelly, J.H. and Evers, J.H., "An Interpolation Strategy for Scheduling Dynamic Compensators," *In Proceedings of the 1997 AIAA Guidance, Navigation, and Control Conference*, New Orleans, USA, 1997, pp. 1682-1690

[22] Kelly, J.H., Evers, J.H., Korn, R.A. and Lawrence, D.A., "Scheduling Dynamic Compensators via Control Signal Interpolation," *In Proceedings of the AIAA Guidance, Navigation, and Control Conference and Exhibit*, Portland, USA, 1999, pp. 176-186.

[23] Nichols, R.A., Reichert, R.T. and Rugh, W.J. "Gain Scheduling for H∞ Controllers: A Flight Control Example," *IEEE Transactions on Control Systems Technology*, Vol.1, No 2, 1993, pp.69-79.

[24] Lin, Z. and Khammash, M., "Robust Gain-scheduled Aircraft Longitudinal Controller Design Using an H∞ Approach," *In Proceedings of the 20th American Control Conference*, , Arlington, USA, 2001, pp. 2724-2729.

[25] Stilwell, D.J. and Rugh, W.J., "Interpolation of Observer State Feedback Controllers for Gain Scheduling," *IEEE Transactions on Automatic Control*, Vol.44, No.6, 1999, pp.1225 1229.

[26] Stilwell, D.J. and Rugh, W.J., (2000), "Stability-preserving Interpolation Methods for the Synthesis of Gain-scheduled Controllers," *Automatica*, Vol. 36, pp.665-671.

[27] Zhou, K., Doyle, J.C. and Glover, K., *Robust and Optimal Control*, Prentice–Hall, Upper Saddle River, NJ, 1996.

[28] Siouris, G.M., *Missile Guidance and Control Systems*, New York, Springer-verlag, Inc, 2004.